



ACADEMIC
PRESS

Available online at www.sciencedirect.com

SCIENCE @ DIRECT®

Journal of Solid State Chemistry 170 (2003) 30–38

JOURNAL OF
SOLID STATE
CHEMISTRY

<http://elsevier.com/locate/jssc>

Control of grain size and morphologies of nanograined ferrites by adaptation of the synthesis route: mechanosynthesis and soft chemistry

N. Guigue-Millot,^{a,*} S. Bégin-Colin,^b Y. Champion,^c M.J. Hÿtch,^c G. Le Caër,^d and P. Perriat^e

^aLaboratoire de Recherches sur la Réactivité des Solides, UMR 5613 CNRS/Université de Bourgogne, BP 47 870, 21078 Dijon Cedex, France

^bLaboratoire de Science et Génie des Matériaux Métalliques, UMR 7584, 54042 Nancy Cedex, France

^cCentre d'Etudes de Chimie Métallurgique, CNRS, 15 rue G. Urbain, 94407 Vitry Cedex, France

^dGroupe Matière Condensée et Matériaux, UMR 6626, Université de Rennes-I, Avenue du Général Leclerc, 35042 Rennes Cedex, France

^eGroupe d'Etudes de Métallurgie Physique et de Physique des Matériaux, INSA de Lyon, 69621 Villeurbanne Cedex, France

Received 1 March 2002; received in revised form 27 June 2002; accepted 5 August 2002

Abstract

Nanocrystalline Fe-based spinels with composition $\text{Fe}_{2.5}\text{Ti}_{0.5}\text{O}_4$ can be synthesized using two different routes: soft chemistry and high-energy ball milling. This paper is focussed on the fact that each type of synthesis process can lead to powders with a crystallite size of about 15 nm but with significant differences in the grain size distribution and the agglomeration state. Whereas in the case of mechanosynthesis, the ball-milled powders consist of aggregates, those obtained by soft chemistry are very well dispersed. Moreover the chosen investigated nanopowders present a blocked/superparamagnetic transition depending on the grain size. The grain size morphologies obtained by the two techniques of synthesis can then be fully characterized by complementary experiments: in addition to high-resolution image processing, specific measurements adapted to the study of magnetic relaxation can be used for weighting differently their small and large size tails: namely, magnetization measurements and Mössbauer spectrometry.

© 2002 Elsevier Science (USA). All rights reserved.

Keywords: Mechanosynthesis; Soft chemistry; Nanoparticles; Spinel; High-resolution transmission electron microscopy; Mössbauer spectrometry

1. Introduction

Nanostructured materials are known to exhibit properties different from those of conventional materials with coarser microstructure. The so-called “nanometric effect” is a major issue of discussion both experimentally and theoretically [1]. However, the influence of synthesis methods on materials properties is rarely considered in the literature. We have previously demonstrated that nanometer-sized titanoferrites synthesized either by mechanical alloying or by soft chemistry display different characteristics [2], namely in: deviations from oxygen stoichiometry, defects, cation distributions, etc. In this paper we investigate differences in the morphology properties, mainly the state of

aggregation and the particle size distribution, originating from the two synthesis techniques. Such differences may strongly influence properties of these nanomaterials. Moreover the nanometer-sized studied titanoferrites present a magnetic relaxation depending on the grain size. This property is, in fact, used here to compare the relevant differences in the morphological characteristics of the powders synthesized by the two techniques. Indeed, in addition to classical grain size characterizations, specific magnetic measurements appropriate for the determination of grain size distributions in aggregated nanometric titanoferrites are used.

Ferrites with spinel structure $\text{Fe}_{3-x}\text{M}_x\text{O}_4$ (M is a cation, $M = \text{Mn}, \text{Zn}, \text{Mo}, \text{V}$, etc and $0 \leq x \leq 1$) have been thoroughly studied over many decades [3]. In these spinel phases, a change of the cation-to-anion ratio leads possibly to a deviation δ from oxygen stoichiometry: $(\text{Fe}_{3-x}\text{M}_x)_{1-\delta}\text{O}_4$ [4]. In the spinel structure, two types of

*Corresponding author.

E-mail address: nmillot@u-bourgogne.fr (N. Guigue-Millot).

sites are available for cations [5]: tetrahedral (A) and octahedral (B). When the considered ferrite contains some M cations, the cation distribution is more complicated than in magnetite where all the Fe^{2+} ions are on B sites. In the case of titanium ferrite, the distribution of cations has been extensively studied using several methods [6–11]. Discrepancies between the reported cation distributions may originate from the different methods of synthesis, the various experimental conditions and control parameters used by different authors, for instance temperature, particle size, deviation from oxygen stoichiometry, etc. In our experimental conditions, we aim at controlling the average grain size of the cubic phase by dissolving titanium into magnetite both to stabilize the spinel structure for high values of δ and to avoid grain growth [2]. The Ti content has been chosen both to be close to that of natural titanomagnetites, $\text{Fe}_{2.4}\text{Ti}_{0.6}\text{O}_4$ [12] and to allow easy synthesis. As previous trials with oxalate precursors showed that the synthesis of titanomagnetites $\text{Fe}_{3-x}\text{Ti}_x\text{O}_4$ with $x \leq 0.5$ was possible [13, 14], we finally selected a Ti content $x = 0.5$ [2]. Nanometer-sized titanoferrites were synthesized by two routes: soft chemistry and mechanochemistry. Among the numerous methods of soft chemistry, we chose the precipitation method which yields large quantities of powder (about 10 g) with nanometer-sized grains [15, 16]. The precipitation step was followed by different treatments to eliminate remaining impurities and to reach a stoichiometric product ($\delta \approx 0$) from $\text{N}_2/\text{H}_2/\text{H}_2\text{O}$ gas mixtures controlled using a specific device previously described [17]. The second synthesis route, mechanochemistry [18–20] was for instance used for the direct synthesis of ferrites [21–23]. However, the formation of a single phase has never been reported except in the case of Ni ferrite. Further, the mechanochemistry times were very long and led to large Cr and Ni contamination (about 9 at%) from milling tools. In this study, by appropriate adjustment of ball-milling energy, the spinel phase was obtained after only 4 h of grinding at room temperature and without significant contamination [2]. Both methods lead to powder particles with nanometer-sized grains of similar mean sizes but with a priori very different powder morphologies.

To describe the grain size distributions of these titanoferrites, techniques appropriate for particles whose sizes range between 5 and 20 nm are required. As grain sizes are in the nanometric range, ferrites which are magnetically ordered may exhibit a superparamagnetic behavior which possibly yield information about grain size distribution. Superparamagnetic relaxation results from a competition between anisotropy energy (KV where K is the anisotropy constant and V the particle volume) and thermal energy $k_B T$ (k_B is the Boltzmann constant and T the temperature) [24]. The effect is further associated to a strong decrease of

some parameters such as the coercivity, H_c . For a given experiment, the occurrence of superparamagnetic relaxation depends both on the respective value of the characteristic measuring time τ_m and on the relaxation time of the magnetic moments

$$\tau = \tau_0 \exp(KV/k_B T) \quad (1)$$

(τ_0 is a constant depending on various parameters).

If $\tau_m \gg \tau$, relaxation is so fast that particles behave like a (super)paramagnetic system. By contrast, if $\tau_m \ll \tau$, relaxation appears so slow that a blocked state (like in a magnetic ordered crystal) is observed [24]. The blocking temperature T_B is defined as the temperature at which $\tau_m = \tau$. For a given size T_B increases with decreasing measuring time, the highest value of T_B being in any case the Curie Temperature T_c . The critical sizes \varnothing_c of the transition block state/superparamagnetic state have been calculated according to relation (1) [24].

The purpose of the present paper is to investigate grain size distributions of two powders of $\text{Fe}_{2.5}\text{Ti}_{0.5}\text{O}_4$ which have approximately the same average grain size. Since in the size range 5–20 nm, the observation of superparamagnetic relaxation not only depends on grain size distribution but also on temperature and on the measuring technique, two different magnetic techniques (magnetometry and Mössbauer spectrometry) were used in addition to electron microscopy techniques (scanning electron microscopy, SEM and high-resolution transmission electron microscopy, HRTEM).

2. Experimental

The experimental conditions of powder synthesis by soft chemistry and by high-energy ballmilling have been described in detail elsewhere [2, 25]. The main steps of the soft chemistry route were (i) dissolution of suitable amounts of ferrous, ferric and titanium chloride in HCl solution, (ii) addition into an ammonia solution stirred at 800 rpm, (iii) washing with deionized water under ultrasonication then separated by centrifugation (4 times), (iv) freeze-drying, (v) calcination under air at 380°C, (vi) thermal treatment at 460°C under 1.4×10^{-24} Pa (obtained from suitable $\text{N}_2/\text{H}_2/\text{H}_2\text{O}$ gas mixtures). The mechanochemically synthesized ferrites were obtained from TiO_2 , Fe_2O_3 and iron powder mixtures after milling for 4 h. Continuous grinding was performed in a Fritsch P7 planetary ball mill (with steel milling tools) with a powder-to-ball weight ratio $R = 1/40$ and under an argon atmosphere.

The resulting powders were characterized by X-ray diffraction (XRD) using a D5000 diffractometer with $\text{CuK}\beta$ radiation. The lattice parameters of the powders were deduced from XRD line positions using a

least-squares refinement method¹. XRD line profile analysis was performed in order to determine grain morphology, average crystallite size (size of a region over which the diffraction is coherent) and crystallographic imperfections (microdistortions, stacking faults, planar defects, etc.) [26]. Pattern decomposition was carried out by means of the profile fitting program PROFILE² to obtain parameters defining the position, height, area, integral width and shape of individual Bragg reflections. The instrumental corrections were obtained from an annealed BaF₂ reference. The experimental profile for the peaks was Voigtian [27] and therefore the broadening was given by the formula

$$\beta^{*2} = \frac{\beta^*}{\varepsilon} + \eta^2 d^{*2}, \quad (2)$$

where β is the integral width, ε the parameter linked to crystallite or domain size and shape (in the case of spherical crystallites, their mean diameter is given by $d = 4/3\varepsilon$) and η the parameter linked to strain (the rate mean strain = $\eta/5$). $\beta^* = \beta \cos \theta / \lambda$ and $d^* = 2 \sin \theta / \lambda$ are the reduced coordinates depending on the diffraction angle θ and on the wavelength λ .

The ⁵⁷Fe Mössbauer spectra (characteristic measuring time $\tau_m \approx 10^{-8}$ s [24]) were recorded in transmission geometry with a spectrometer operated in a constant acceleration mode and a ⁵⁷Co source in Rh with a strength of about 10 mCi.

The hysteresis loops of samples (characteristic measuring time $\tau_m \approx 1 - 100$ s [24]) were measured with an M2100 50 Hz hysteresometer.

HRTEM was carried out using a TOPCON 002B microscope operating at 200 kV ($C_s = 0.4$ mm, nominal resolution 1.85 Å). The HRTEM images were digitized and an analysis of the variations in structure was performed using the geometric phase technique explained elsewhere [25, 28]. The phase images are calculated from the digitized HRTEM images by Fourier filtering (image processing was carried out using procedures written within the image processing package DigitalMicrograph 2.5, Gatan Inc.).

3. Results and discussion

As shown in Fig. 1a, powders prepared by soft chemistry, named hereafter “soft chemistry powders” for brevity, are in the nanometric scale and homogeneous with a particle size of about 15 nm. This value matches quite well with the average particle diameter deduced from specific area measurements (Table 1) and the crystallite size deduced from XRD results

$\varnothing_{\text{XRD}} = 18$ nm. Fig. 1 illustrates that SEM analysis does not allow any distinction between the two powders: according to this technique, they both have a crystallite size of about 15 nm. Nevertheless, the combination of specific area measurements and XRD diffraction analyses (Table 1) demonstrates that the soft chemistry powder is very well dispersed; in contrast, mechano-synthesized powder consists of aggregates of nanometric crystallites. The average size of the aggregates is approximately 300 nm (Table 1) and the size of small crystallites in aggregates is about 10–15 nm (Fig. 1b and Table 1). These results show that soft chemistry powders are finely dispersed whereas ball-milled powders are highly aggregated.

The grain size distribution of these nanometric ferrites was characterized using a combination of several techniques with different measuring times such as magnetization measurements, Mössbauer spectrometry and from high-resolution image processing.

3.1. Determination of powders morphology from high-resolution electron micrographs

Scanning electron micrographs (Figs. 1a and b) suggest that the particle size distribution of the ball-milled powder is broader than that of the powder obtained by soft chemistry. To characterize better the powder microstructures, powders have been examined by HRTEM. As observed in Fig. 2, the soft chemistry powder is very well dispersed with individual grains clearly seen by HRTEM (Fig. 2a). By contrast, the mechano-synthesized powder shows grains which are entangled and difficult to distinguish separately (Fig. 2b). The contrast variations in the phase image of the previous micrographs were then analyzed. A uniform gray level corresponds to a given orientation and a given periodicity [25, 28]. Crystallites of sizes lower than 10 nm and others of sizes equal to 20 nm were identified in the mechano-synthesized powder (see examples in Fig. 2). Crystallites of mechano-synthesized powders were found to have a smaller average size than those obtained by soft chemistry but seem to present a broader size distribution. This is in agreement with the analyses of XRD patterns which show that the diffraction lines of the ball-milled powder have a “super-Lorentzian” shape usually attributed to size effects: each diffraction line is in fact the sum of Gaussian profiles (normally associated with broadening originating from defects) with very different widths each one corresponding to different crystallite sizes [29]. Such a “super-Lorentzian” profile seems to be a characteristic of mechano-synthesized materials.

Finally, except for few grains in soft chemistry powders with hexagonal shape, the grains were approximately spherical in both powders.

¹In-house software taking into account the effect of sample gap.

²Available in the PC software package DIFFRACT AT supplied SIEMENS.

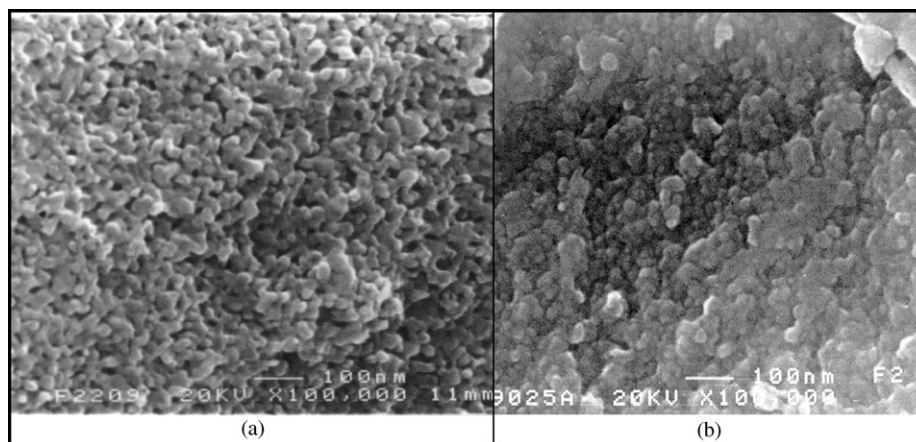


Fig. 1. SEM micrograph of $\text{Fe}_{2.5}\text{Ti}_{0.5}\text{O}_4$ synthesized by (a) soft chemistry (reduction at 460°C , $p\text{O}_2 = 8 \times 10^{-27}$ Pa) and (b) mechanosynthesis (4 hs, $R = 1/40$, under argon).

Table 1

Specific area measurements and XRD analyses of $\text{Fe}_{2.5}\text{Ti}_{0.5}\text{O}_4$ synthesized by soft chemistry (reduction at 460°C , $p\text{O}_2 = 8 \times 10^{-27}$ Pa) and mechanosynthesis (4 h, $R = 1/40$, under argon). The XRD line profile analysis is performed according to the Williamson and Hall method, the determination of the lattice parameter is based on a least-squared refinement method.

Powder	Specific area (m^2/g)	BET \varnothing (nm)	DRX \varnothing (nm)	Strain	Lattice constant a (\AA)
Soft chemistry	68 ± 2	17.6 ± 0.3	18 ± 2	0.000	8.424 ± 0.001
Mechanosynthesis	4.1 ± 0.5	279 ± 5	12 ± 2	0.021	8.465 ± 0.001

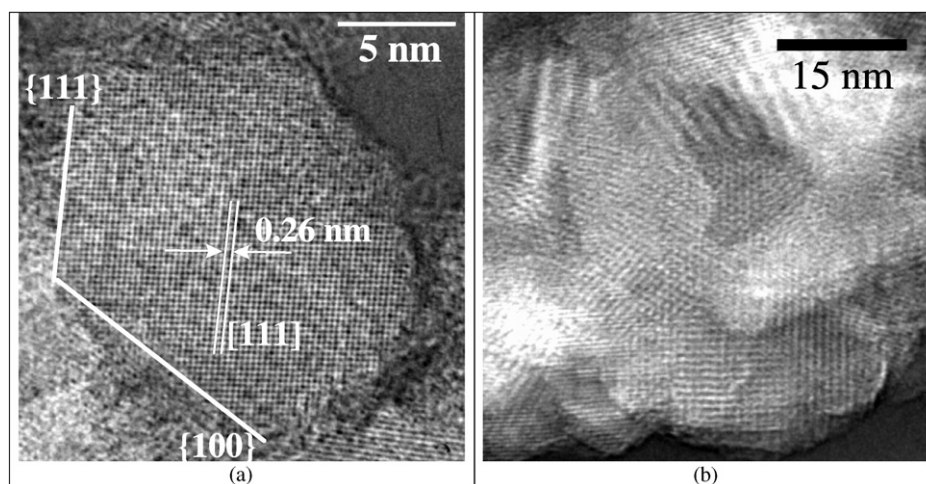


Fig. 2. HRTEM micrograph of $\text{Fe}_{2.5}\text{Ti}_{0.5}\text{O}_4$ synthesized by (a) soft chemistry (reduction at 460°C , $p\text{O}_2 = 8 \times 10^{-27}$ Pa) and (b) mechanosynthesis (4 hs, $R = 1/40$, under argon).

3.2. Determination of the powder morphology by studying hysteresis loops at ambient temperature

The measurement of hysteresis loops at ambient temperature revealed (Fig. 4) three main differences between powders obtained by mechanosynthesis and by soft chemistry: their loop shapes, their magnetizations in a given field and their coercive fields.

The hysteresis loop of the powder obtained by soft chemistry is closer to a square than that of the ball-milled powder. The square shape is characteristic of a material with high magnetic susceptibility (that is to say which easily magnetizes). This first difference suggests that the mechanosynthesized powder contains a large number of particles whose sizes are significantly smaller than those of soft chemistry powders. Indeed, when

particle sizes become smaller than some threshold between the superparamagnetic state and the blocked state, \varnothing_c^{DC} , powders magnetized very hardly [24]: for a particle of volume V , the free energy of interaction between its magnetization M and the external field H_{ext} ($-MH_{ext}V$) may become negligible compared to the thermal energy ($k_B \times T$) when V decreases. Contrary to the powder obtained by soft chemistry, a significant fraction of particles of the ball-milled powder had then a grain size lower than $\varnothing_c^{DC} \approx 17$ nm (the critical grain size at room temperature for a Fe_3O_4 sample, value given in the reference [24]). For the soft chemistry powder, the shape of the hysteresis loop suggests that there was only a negligible fraction of particles of size lower than \varnothing_c^{DC} .

These results are in agreement with the size homogeneity of the soft chemistry powder, inferred from XRD experiments and SEM (Fig. 1). In this interpretation, the magnetic dipolar interactions between the particles have been neglected. It is justified by the fact

that these interactions, often leading to a collective state with spin glass-type properties, are more usually observed in nanometric ferromagnetic metallic particles assemblies [30,31]. For $\gamma-Fe_2O_3$ particles in a polymer, J.L. Dormann [2, p. 330, E 2.5.] has demonstrated that “the relaxation rate is almost the same for samples showing negligible, weak and strong interactions... the regime is the same for all samples and no collective state appears”.

These differences between the two grain size distributions may also be quantified by comparing the magnetizations of the two powders measured at room temperature in a field of 6000 Oe. The values must first be normalized with respect to the calculated values of the saturation magnetization at 0 K which are, respectively, 33 emu/g for the soft chemistry powder and 54 emu/g for the ball-milled powder. The theoretical magnetizations were calculated by using, on the one hand, the usual values of magnetic moments of Fe^{2+} cations ($4.3 \mu_B$) and of Fe^{3+} cations ($5 \mu_B$) [32] and, on

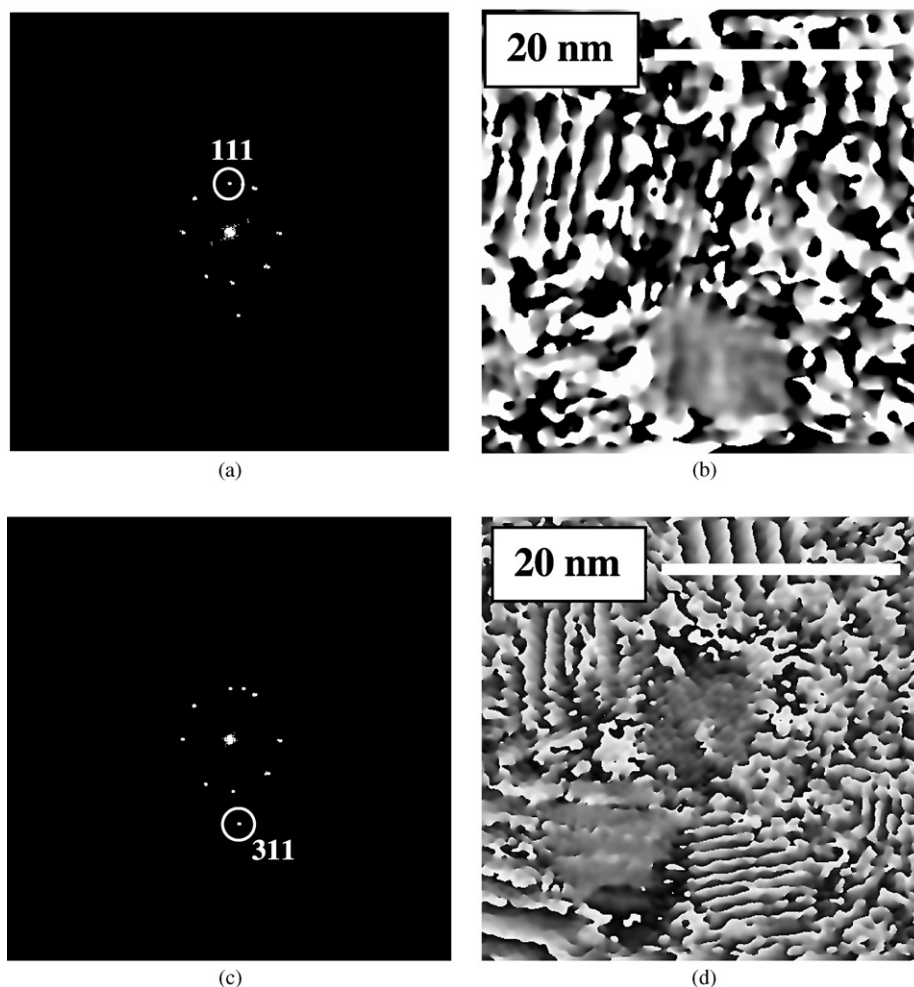


Fig. 3. HRTEM image analysis of an $(Fe_{2.5}Ti_{0.5})O_4$ titanium ferrite powder prepared by mechanochemistry. (a), (c), (e), (g): Fourier transform of Fig. 2b. Circles show the filtering of the (kkl) lattice fringes. (b), (d), (f), (h): (hkl) phase image calculated by Fourier filtering: $P_{hkl}(r)$, black = 0 white = 2π . A uniform gray correspond to a same crystallographic orientation and a regular lattice constant. Some crystallites sizes are lower than 10 nm, others are equal to 20 nm.

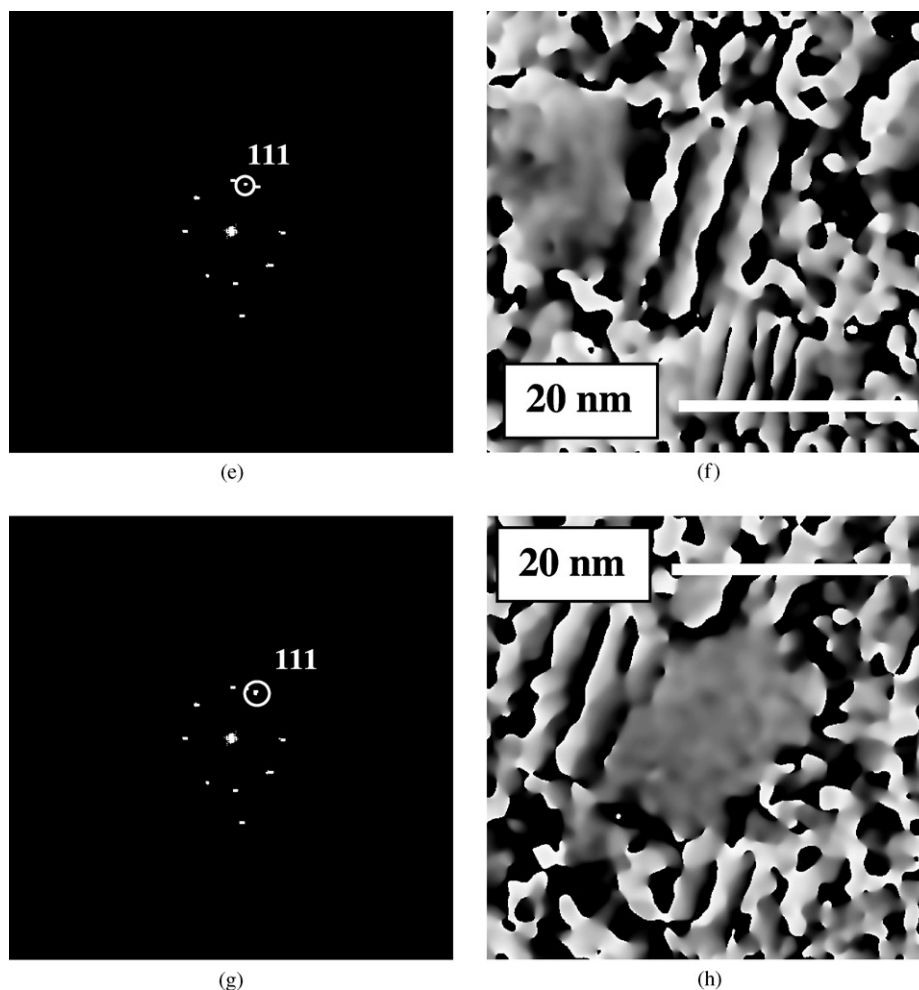


Fig. 3 (continued).

the other hand, the cation distributions determined previously [2]. This calculation is justified thanks to neutron diffraction experiments not yet published. Indeed, the lack of the 422 reflection proves that the ferrimagnetism is collinear. For the soft chemistry powder, the experimental value is consistent with that calculated (33 emu/g) despite the fact that the measurement was made at ambient temperature and that saturation was not reached. This reinforces our conclusion that the sizes of most grains of soft chemistry powders are larger than 17 nm. By contrast, there is a strong difference between the experimental (17 emu/g at room temperature) and the calculated (54 emu/g at 0 K) values of the magnetization of the ball-milled sample. If we assume that only the grains which are in the magnetically blocked state contribute significantly to the measured magnetization and that these particles have consequently sizes larger than 17 nm, we estimate from Fig. 4 that roughly 1/5 of grains of mechanosynthesized powders have a size larger than 17 nm.

These results (especially the larger heterogeneity of the mechanosynthesized powders) are confirmed by the

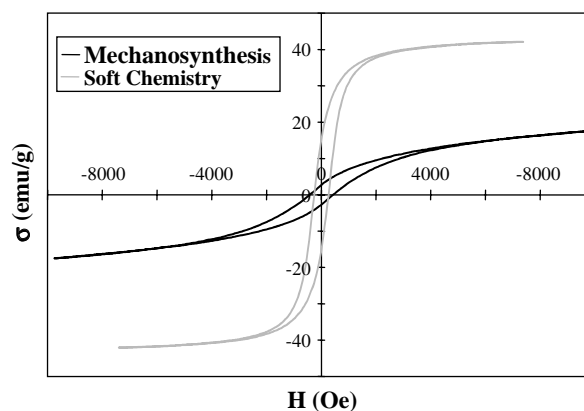


Fig. 4. Hysteresis cycle of $\text{Fe}_{2.5}\text{Ti}_{0.5}\text{O}_4$ synthesized by soft chemistry (reduction at 460°C , $p\text{O}_2 = 8.10^{-27}$ Pa) and mechanosynthesis (4 h, $R = 1/40$, under argon). Ball-milled powder magnetization is incomplete due to smaller particles.

values of the coercive fields. Indeed, only the grains in the blocked state, i.e., of size larger than 17 nm, are expected to present significant hysteresis. However, the coercivity value of 430 Oe for the mechanosynthesized

titanomagnetite is almost twice that of the soft chemistry powder (270 Oe). The higher coercive field value for the mechanothesized powder may be due to a larger proportion of structural defects and due to the presence of magnetostrictive cations: Fe_A^{2+} cations in tetrahedral coordination [33]. However, the most probable contribution to such a high-field value comes from grains with large sizes. Even if there are 5 times less grains of size larger than 17 nm in the mechanothesized powder, these grains would have an average size larger than those of soft chemistry powders. Coercive field measurements, which allow probing the large-size side of the distributions of grain sizes ($\varnothing > \varnothing_c^{\text{DC}} \approx 17$ nm), confirm thus that the latter distribution is much broader for mechanothesized powders than it is for soft chemistry powders.

To conclude, magnetic measurements, which are on the whole sensitive both to the small-size and the large-size end of the distributions of grain sizes, confirm that the mechanothesized powders have a size distribution much broader than that of the soft chemistry powders, possibly with a tail extending significantly to large sizes.

3.3. Determination of the powder morphology by Mössbauer spectrometry: comparison of two techniques with different measuring times

A tentative semi-quantitative approach yields the typical grain diameter below which superparamagnetism is observed as with Mössbauer spectrometry $\varnothing_c^{\text{Mössbauer}} \approx 9$ nm (at room temperature), being thus smaller than the corresponding size for DC measurements $\varnothing_c^{\text{DC}} \approx 17$ nm. The critical sizes \varnothing_c of the transition block state/superparamagnetic state have been calculated according to the relation (1) where τ is the relaxation time, k_B the Boltzmann constant, T the temperature, K the anisotropic constant and V the particle volume [24]. $K = 4.4 \times 10^{-2}$ J/cm³ (value of a Fe_3O_4 sample [24]), $\tau/\tau_0 = 66.5$ (value of the literature [24]: $\tau_m = 10^{-8}$ s for Mössbauer experiments and $\tau_0 \approx 10^{-10}$ s) have been chosen. Very different values of anisotropic constant have been published for similar titanium compositions: K_1 (294 K) = 2×10^{-3} J/cm³ for a single crystal $\text{Fe}_{2.4}\text{Ti}_{0.6}\text{O}_4$ [34], K_1 (298 K) = -3×10^{-4} J/cm³ for a synthetic $\text{Fe}_{2.4}\text{Ti}_{0.6}\text{O}_4$ powder (composition analogue of magnetic minerals) [35], K_1 (295 K) $\approx -1.2 \times 10^{-2}$ and -0.5×10^{-2} J/cm³, respectively for Fe_3O_4 and $\text{Fe}_{2.5}\text{Ti}_{0.5}\text{O}_4$ single crystals [36]. K_2 (295 K) $\approx 1.35 \times 10^{-2}$ J/cm³ for a $\text{Fe}_{2.45}\text{Ti}_{0.55}\text{O}_4$ single crystal [36]. The differences may originate from synthesis conditions, cationic distribution or lattice strain. In any case, there is a strong $K_1(x)$ dependence for $x > 0.5$ which can explain the low K_1 values published for titanium ferrites with a composition close to that of natural titanomagnetite [34, 35]. For $x = 0.5$, the value

of K_1 is very close to that of $x = 0$, so the value of Dormann for a Fe_3O_4 sample ($K = 4.4 \times 10^{-2}$ J/cm³ [24]) can be chosen for theoretical calculations in this paper.

Even if few differences exist between the spectrum of a ferrite with the same composition as ours [37, 38] and the ^{57}Fe Mössbauer spectrum of the spinel phase synthesized by soft chemistry, Fig. 5a, the latter is the one expected for a ferrite in a magnetic blocked state [39]. This is consistent with the mean grain size of the soft chemistry powder, with the size distribution and consequently with a negligible fraction of grains with a size < 9 nm. The room temperature spectrum of the ferrite obtained by mechanothesized, Fig. 5b₁, is composed of a “sextuplet” whose only four very broad external lines are visible and of an intense asymmetrical central doublet. The Mössbauer spectra recorded at room temperature and below (100 and 200 K [2]) are complex with shapes evolving with temperature as do spectra typical of magnetic relaxation ([24] and references therein). The central doublet appears to be more symmetric at 200 K than it does at room temperature. The velocity interval between the two “peaks” increases slightly as expected, from about 1.65 to about 1.85 mm/s, between room temperature and 200 K. An interpretation which would attribute part of the central doublet to a separate Fe^{2+} phase, which would be magnetic with a transition temperature $T_c = 200$ K, can be ruled out. The latter hypothetical phase would indeed represent a significant fraction of the sample and is not detected from X-ray and electron diffraction patterns. Despite the fact that the spectra cannot be interpreted in detail as grains are further expected to interact magnetically in mechanothesized powders, some information can nevertheless be obtained. The spectral shape at room temperature is typical of the shape obtained for a broad size distribution as seen from Fig. F6.8 of [24]. The lognormal distribution has often been found to be a reasonable approximation of actual grain sizes distributions. Assuming grains to be spherical with a diameter d , the lognormal probability density $\rho(d)$ is given by

$$\rho(d) = \frac{1}{d\sigma\sqrt{2\pi}} \exp \left\{ -\frac{(\log d - \log D)^2}{2\sigma^2} \right\} \quad (3)$$

or equivalently $\log d$ has a Gaussian distribution with a mean $\log D$ and a standard deviation σ . The lognormal distribution, which depends only on two parameters, is used here to yield estimates of the fraction of particles with a diameter less or greater than the prescribed sizes. Knowing that $\langle d \rangle = 12$ nm and that there are about 20% of particles with $d > 17$ nm, we select $D = 9.2$ nm and $\sigma = 0.73$ nm. About 50% of the particles are then expected to have a diameter $d \leq 9$ nm, in agreement with the Mössbauer spectrum (Fig. 5b₁), which shows that about 50% of the spectral area is indeed associated with the magnetically split broad component.

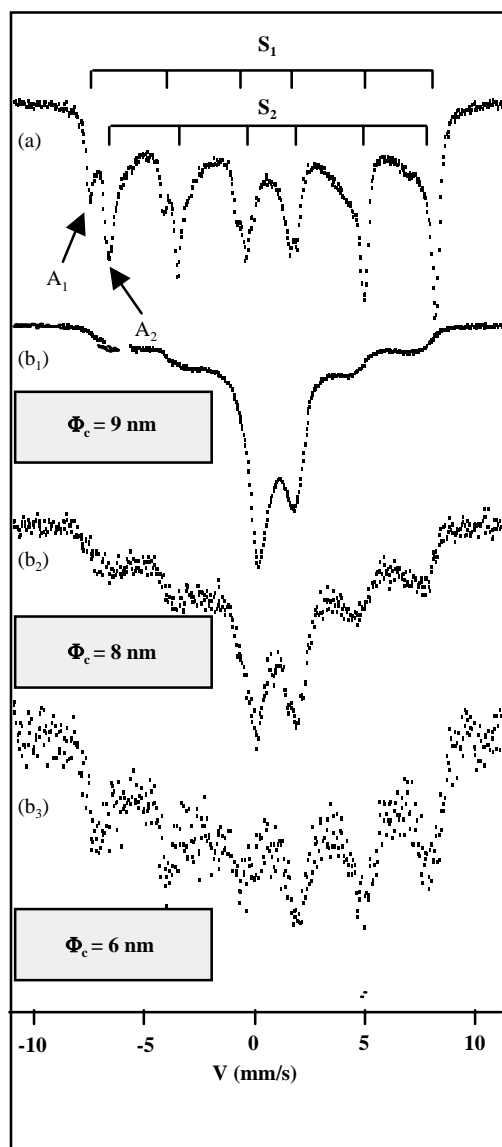


Fig. 5. (a) Room temperature ^{57}Fe Mössbauer spectra of $\text{Fe}_{2.5}\text{Ti}_{0.5}\text{O}_4$ synthesized by soft chemistry (reduction at 460°C , $p\text{O}_2 = 8 \times 10^{-27}$ Pa). It displays several sextets, the outer subspectrum S_1 whose field is easily calculated is related to Fe^{3+} at A sites with a typical hyperfine field H_1 of 48.6 ± 0.25 T. The subspectrum S_2 has an average field H_2 of 45.5 ± 0.25 T. A noticeable characteristic is the asymmetry of the groups of lines A_1 and A_2 . The first absorption minimum A_1 on the negative velocity side around -8 mm/s looks indeed much smaller than the next minimum A_2 around -7 mm/s. (b) ^{57}Fe Mössbauer spectra of $\text{Fe}_{2.5}\text{Ti}_{0.5}\text{O}_4$ synthesized by high-energy ball milling (4 h $R=1/40$, under argon): (b₁) room temperature spectra, (b₂) 200 K spectra and (b₃) 100 K spectra. The critical sizes Φ_c of the transition block state/superparamagnetic have been calculated thanks to the relation $\tau = \tau_0 \exp(KV/k_B T)$ where τ is the relaxation time, k_B the Boltzmann constant, T the temperature, K the anisotropic constant and V the particle volume [24]. $K = 4.4 \times 10^{-2}$ J/cm³ (value of an Fe_3O_4 sample [24]), $\tau/\tau_0 = 66.5$ (value of the literature [24]; $\tau_m = 10^{-8}$ s for Mössbauer experiments and $\tau_0 = 10^{-10}$ s) have been chosen.

The changes of spectra when the temperature decreases confirm the occurrence of superparamagnetic relaxation, which is in turn consistent with an average

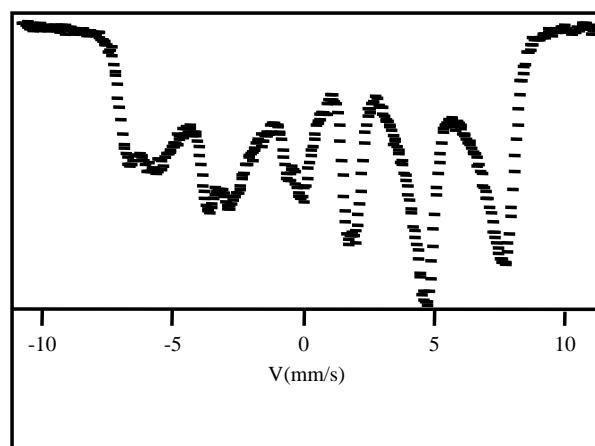


Fig. 6. ^{57}Fe room temperature Mössbauer spectra of $\text{Fe}_{2.5}\text{Ti}_{0.5}\text{O}_4$ synthesized by mechanosynthesis (4 h, $R=1/40$, under argon) and annealed at 800°C .

crystallite size of 12 nm for the ball-milled powder (Fig. 5b₂ and b₃). The broad distribution of grain size results in a broad distribution of blocking temperatures: the bigger a grain, the higher its blocking temperature [24]. The hyperfine field calculated from the two intense outer lines is 46.5 ± 0.5 T at 100 K, a value quite consistent with an Fe^{3+} field at low temperature. A field of about 45 T is indeed calculated from the Mössbauer spectrum at 90 K of $\text{Fe}_{2.3}\text{Ti}_{0.7}\text{O}_4$ [37]. The spectrum at 100 K still reflects the effects of a significant superparamagnetic contribution which is again consistent with the large width of the size distribution of mechanosynthesized powders. This conclusion is consistent with those obtained from the high-resolution transmission microscopy analysis (Fig. 3). The crystallite size distribution in titanoferrites prepared by soft chemistry has a slightly larger mean but is significantly narrower than the size distribution in mechanosynthesized ferrites. This explains why a superparamagnetic behavior, which originates from the smallest crystallites, is clearly observed only in the latter case.

Mössbauer spectra show further that the hyperfine field calculated from the external lines which originate from particles in the blocked state remains at about (43.5 ± 1) T when the temperature decreases, that is when the fraction of grains in the blocked state becomes larger and larger (Fig. 5b₁–b₃). Moreover, we measured a hyperfine field of (43.5 ± 1.5) T in $\text{Fe}_{2.5}\text{Ti}_{0.5}\text{O}_4$ with coarse grains in agreement with published values [37, 38]. Finally, the room temperature hyperfine field of the external sextuplet of a ball-milled powder annealed in an inert atmosphere at 800°C is 45.5 ± 0.5 T (Fig. 6). As hyperfine fields depend sensitively on the titanium content, we conclude that Mössbauer spectra of as-milled powders reflect basically the occurrence of magnetic relaxation in grains with a broad size distribution and with a narrow composition distribution.

4. Conclusions—Powders obtained by mechanosynthesis and soft chemistry: two powders in the nanometric range but with strongly different morphologies

Electron microscopy observations, hysteresis loop measurements and Mössbauer spectrometry make it possible to conclude without ambiguity that soft chemistry lead to well-dispersed particles with a narrow grain size distribution. On the contrary, mechanosynthesized powders with a slightly smaller mean size (12 nm) consist of aggregated particles with a broad grain size distribution which extends from less than 9 nm to more than 17 nm. Such quantitative conclusions about the differences of the powders synthesized by the two techniques mainly originate from the magnetic particularities of the sample investigated. More precisely, they were made possible by the study of the grain size dependency of the superparamagnetic relaxation transition using different techniques with different characteristic measuring times. In a previous paper, the composition of particles obtained by soft chemistry was shown to exhibit changes of the valences of cations and of their nature from the bulk to the surface of particles. The combination of both results (grain size/composition heterogeneity) explains the difficulties of synthesizing almost perfect nanometer-sized particles: interactions between particles through aggregation seem to be the only possibility to avoid such composition gradients inside each particle but, at the same time, they appear to imply the occurrence of heterogeneities in both particle size and morphology. Obtaining simultaneous homogeneity in both morphological and chemical properties is then the challenge in nano-chemistry of multi-component samples.

Acknowledgments

The authors thank P. Delcroix, Dr. M. Guyot and Prof. B. Malaman for their help in the experiments.

References

- [1] R.P. Andres, R.S. Averback, W.L. Brown, L.E. Brus, W.A. Goddard, A. Kaldor, S.G. Louie, M. Moscovits, P.S. Peercy, S.J. Riley, R.W. Siegel, F. Spaepen, Y. Wand, *J. Mater. Res.* 4 (1999) 704.
- [2] N. Millot, S. Bégin-Colin, P. Perriat, G. Le Caër, *J. Solid State Chem.* 139 (1998) 66.
- [3] B. Gillot, *J. Solid State Chem.* 113 (1994) 163.
- [4] R. Dieckmann, *Ber. Bunsenges. Phys. Chem.* 86 (1982) 112.
- [5] E.J. Verwey, E.L. Heilman, *J. Chem. Phys.* 15 (1947) 174.
- [6] S. Akimoto, *J. Geomagn. Geoelectr.* 61 (1954) 1.
- [7] L. Néel, *Adv. Phys.* 4 (1955) 191.
- [8] R. Chevalier, J. Bolfa, S. Mathiew, *Bull. Soc. Fr. Mineral Cristallogr.* 78 (1955) 307.
- [9] W. O'Reilly, S.K. Banerjee, *Phys. Lett.* 17 (1965) 237.
- [10] A. Trestman-Matts, S.E. Dorris, S. Kumarakrishnan, T.O. Mason, *J. Am. Ceram. Soc.* 66 (1983) 829.
- [11] H.S.C. O'Neill, A. Navrotsky, *Am. Mineral.* 68 (1983) 181.
- [12] W. O'Reilly, *J. Magn. Magn. Mater.* 137 (1994) 167.
- [13] B. Gillot, F. Jemmal, *React. Solids* 2 (1986) 95.
- [14] B. Gillot, F. Jemmal, *Mater. Chem. Phys.* 15 (1986) 577.
- [15] J.P. Jolivet, *De la solution à l'oxyde*, InterEditions/CNRS Editions, Paris, 1994.
- [16] A. Rousset, F. Chassagneux, *J. Paris, J. Mater. Sci.* 21 (1986) 3111.
- [17] D. Aymes, N. Millot, V. Nivoix, P. Perriat, B. Gillot, *Solid State Ionics.* 101–103 (1997) 261.
- [18] C. Suryanarayana, *Prog. Mater. Sci.* 46 (2001) 1.
- [19] V.V. Boldyrev, N.Z. Lyakhov, Pavlyukhin, E.V. Boldyreva, E.Y. Ivanov, E.G. Avvakumov, *Sov. Sci. Rev. B. Chem.* 14, (1990) 105.
- [20] J.J. De Barbadillo, *Key Eng Mater.* 77–78 (1993) 187.
- [21] G. Concas, F. Congiu, A. Corrias, C. Muntoni, G. Paschina, D. Zedda, *Z. Naturforsch.* 51a (1996) 915.
- [22] C. Jovalekic, M. Zdujic, A. Radakovic, M. Mitric, *Mater. Lett.* 24 (1995) 365.
- [23] W.A. Kaczmarek, M. Giersig, *J. Phys. IV France* 7, (1997) Colloque C1.
- [24] J.L. Dormann, D. Fiorani, E. Tronc, *Adv. Chem. Phys. XCVIII* (1997) 283.
- [25] N. Guigue-Millot, Y. Champion, M.J. Hÿtch, F. Bernard, S. Bégin-Colin, P. Perriat, *J. Phys. Chem.* 105 (29) (2001) 7125.
- [26] J.I. Langford, National Institute of Standards and Technology, Special Publication, Vol. 846, (1992) p. 145.
- [27] N.C. Halder, C.N.J. Wagner, *Adv. X-ray Anal.* 9 (1966) 91.
- [28] M.J. Hÿtch, E. Snoeck, R. Kilaas, *Ultramicroscopy* 74 (1998) 131.
- [29] J.I. Langford, D. Louër, P. Scardi, *J. Appl. Crystallogr.* 33 (2000) 964.
- [30] G. Herzer, *IEEE Trans. Magn.* 26 (1990) 1397.
- [31] G. Herzer, *J. Magn. Magn.* 157/158 (1996) 133.
- [32] J.C. Bernier, P. Poix, *Ann. Chim.* 2 (1967) 81.
- [33] M.P. Sharrock, *IEEE Trans. Magn.* 25 (1989) 4374.
- [34] S. Sahu, B.M. Moskowitz, *Geophys. Res. Lett.* 22 (1995) 449.
- [35] A.P. Brown, W. O'Reilly, *Phys. Earth Planet. Inter.* 116 (1999) 19.
- [36] Z. Kakol, J. Sabol, J.M. Honig, *Phys. Rev. B* 44 (1991) 2198.
- [37] H. Tanaka, M. Kono, *J. Geomagn. Geoelectr.* 39 (1987) 463.
- [38] K. Melzer, Z. Simsa, M. Lukaslak, J. Suwalski, *Cryst. Res. Technol.* 22 (1987) 132.
- [39] U. Russo, S. Carbonin, A. Della Giusta, *Mössbauer Spectroscopy Applied to Magnetism and Materials Science. Vol. 2*, Plenum Press, New York, (1996), p. 207.